# Magnetic properties close to the quantum critical point in YbRh2Si2

**Philipp Gegenwart, Y. Tokiwa, J. Custers, C. Geibel, F. Steglich**

# Magnetic properties close to the quantum critical point in YbRh$_2$Si$_2$

P. Gegenwart[*] , Y. Tokiwa[†] , J. Custers, C. Geibel and F. Steglich

*Max-Planck Institute for Chemical Physics of Solids, D-01187 Dresden, Germany*

The tetragonal heavy fermion system YbRh$_2$Si$_2$ is located very close to a magnetic quantum critical point, related to the suppression of weak antiferromagnetic ordering by a magnetic field of 0.06 T applied in the easy plane perpendicular to the $c$-axis. Here, we report low-temperature measurements of the magnetic ac-susceptibility and dc-magnetization. A pronounced easy-plane anisotropy in the susceptibility indicates that the tetragonal $c$-axis is the magnetic hard direction. For fields $B \perp c$, the isothermal magnetization shows a kink-like structure whose position in field increases with increasing temperature. Corresponding anomalies are observed in the temperature dependence of the ac-susceptibility as well and a new line of anomalies in the temperature-field phase diagram, derived from these experiments, is discussed.

## 1. Introduction

The ground-state behavior of $4f$-based heavy fermion (HF) metals is determined by the interplay of two competing interactions which both depend on the strength of $4f$-conduction electron hybridization $J$.[1] Whereas the Kondo interaction leads to a screening of the local moments, resulting in a paramagnetic ground state with itinerant $4f$-electrons, the indirect exchange coupling (RKKY-interaction) can mediate long-range ordering. By the variation of $J$, these systems can be tuned continuously from the non-magnetic HF state through a magnetic quantum critical point (QCP) into a long-range magnetically ordered state. The important question arises whether the heavy quasiparticles retain their itinerant character and form a spin-density wave (SDW) at the QCP or, alternatively, decompose due to the destruction of the Kondo screening.[2] In the latter case the magnetic order is caused by localized $4f$-electrons that do not contribute to the Fermi surface.

In recent years, the tetragonal YbRh$_2$Si$_2$[3] has become a prototypical system for the study of quantum critical phenomena. It is a HF metal with a characteristic Kondo temperature of $T_K = 25$ K which shows very weak antiferromagnetic (AF) ordering at $T_N = 70$ mK. The partial substitution of Si- with the isoelectronic but larger Ge-atoms in YbRh$_2$(Si$_{1-x}$Ge$_x$)$_2$ with a nominal Ge concentration $x = 0.05$, suppresses the Néel temperature down to 20 mK, without a dramatic increase of the residual resistivity.[4] It has been shown, that magnetic fields are ideally suited for tuning this material as close as possible to the QCP, where the most intense effects of quantum criticality can be studied.[4, 5] When approaching the QCP at the critical field by reducing the temperature from above 1 K to below 20 mK, pronounced non-Fermi liquid behavior is observed: the temperature dependent part of the electrical resistivity follows a linear dependence, $\Delta\rho(T) \propto T$,[3, 5] whereas the electronic specific heat coefficient diverges stronger than logarithmic, i.e. $C_{el}/T \propto T^\alpha$ with $\alpha \approx 1/3$ (Ref.[4]). This behavior is incompatible with the predictions of the itinerant SDW scenario for an AF QCP in both two or three dimensions. Temperature over magnetic field scaling in both of these properties indicates that the characteristic energy of the heavy quasiparticles vanishes at the QCP.[4] This suggests a destruction of the Kondo resonance in accordance with the locally-critical scenario for the QCP. The fractional exponent $\epsilon \approx 0.7$ of the Grüneisen ratio divergence, $\Gamma \propto T^\epsilon$, also demonstrates the failure of the itinerant scenario.[6] Recently, the Hall-effect evolution across the QCP has been studied in great detail at low temperatures.[7] Most remarkably, the suppression of the tiny magnetic ordering with an ordered moment of about $10^{-3}\mu_B$/Yb[8] by magnetic field leads to a large (about 30%) change of the Hall coefficient. A new line in the temperature-field phase diagram has been discovered, across which the isothermal Hall-resistivity as a function of the applied magnetic field changes. Upon decreasing the temperature this feature sharpens, suggesting for the zero-temperature extrapolation a sudden change of the Fermi surface at the QCP.[7]

In this paper, we discuss the low-temperature magnetic properties of YbRh$_2$Si$_2$ (and its slightly Ge-doped version) in the region of the $B - T$ phase diagram very close to the QCP. After giving details concerning experimental techniques (section 2), we first concentrate on results of ac-susceptibility measurements (section 3) which agree very well with the results of the differential susceptibility derived from the dc-magnetization (section 4). Distinct anomalies in their temperature and field dependences are observed. We also focus on the magnetization behavior perpendicular to the easy magnetic plane, i.e. parallel to the $c$-axis. Furthermore, the temperature dependence of the magnetization is compared with that of corresponding $^{29}$Si-NMR Knight-shift measurements. In section 5, the temperature-field phase diagram derived from the magnetic properties is discussed. The summary is presented in section 6.

[*]E-mail address: gegenwart@cpfs.mpg.de

[†]present address: Los Alamos National Laboratory, Condensed Matter and Thermal Physics MST-10, MS K764 Los Alamos, New Mexico 87545, USA

## 2. Experimental

High-quality single crystalline platelets of pure ($x = 0$) and Ge-doped (nominal concentration $x = 0.05$) YbRh$_2$(Si$_{1-x}$Ge$_x$)$_2$ were grown from In flux as described earlier.[3,6] The actual Ge-concentration is estimated to be $x_{eff} = 0.02 \pm 0.004$. The large difference between nominal and actual Ge-concentration arises from the difference in solvability in the In flux between Ge and Si. Residual resistivities of pure and Ge-doped single crystals amount to 1 and 5 $\mu\Omega$cm, respectively. Magnetic ac-susceptibility experiments have been performed with a low-frequency (16.67 Hz) modulation of 0.1 mT.[5] Constant fields have been superposed using a superconducting magnet. For dc-magnetization measurements a high-resolution capacitive Faraday-magnetometer has been utilized.[9]
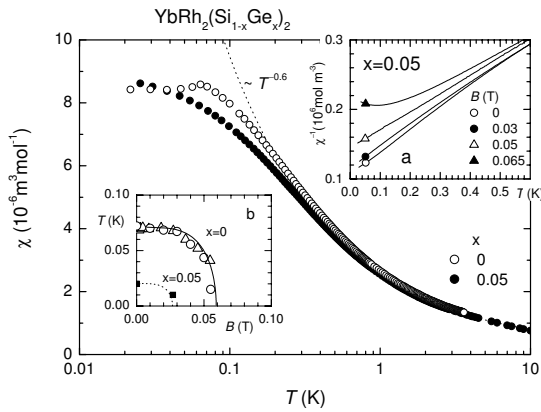
## 3. AC-Susceptibility



Fig. 1. Low-frequency ac-susceptibility $\chi$ vs $T$ of YbRh$_2$(Si$_{1-x}$Ge$_x$)$_2$ (open circles: $x = 0$, closed circles: $x = 0.05$) Dotted line indicates $T^{-0.6}$ dependence. Inset a: $\chi^{-1}$ at various superposed static fields applied perpendicular to the $c$-axis for $x = 0.05$. Inset b: boundary of antiferromagnetic phase for $x = 0$ (open circles from Ref.[5] include resistivity measurements for $B \parallel c$ for which field values have been divided by factor of 11) and $x = 0.05$ (zero-field $T_N$ from specific heat,[4] critical field at 10 mK from magnetostriction[11]).

At first, we focus on ac-susceptibility measurements without superposed static field, displayed in the main part of Fig. 1. At high temperatures, the susceptibility of the pure and Ge-doped system is similar and shows a strong increase upon cooling from 10 K. This increase can be described by a $T^{-0.6}$ dependence that would suggest a ferromagnetic instability close to zero temperature.[10] However, below about 0.3 K, $\chi(T)$ tends towards saturation for both systems and follows a Curie-Weiss (CW) law with a Weiss temperature of about $-0.3$ K indicative for dominating AF fluctuations. For undoped YbRh$_2$Si$_2$, this behavior holds down to $T_N \simeq 70$ mK at which temperature a sharp peak occurs,[4] whereas for the Ge-doped system no deviation from CW behavior is observed down to 25 mK (cf. inset a of Fig. 1). Corresponding specific heat measurements have shown, that $T_N \simeq 20$ mK for YbRh$_2$(Si$_{0.95}$Ge$_{0.05}$)$_2$.[4] The more than



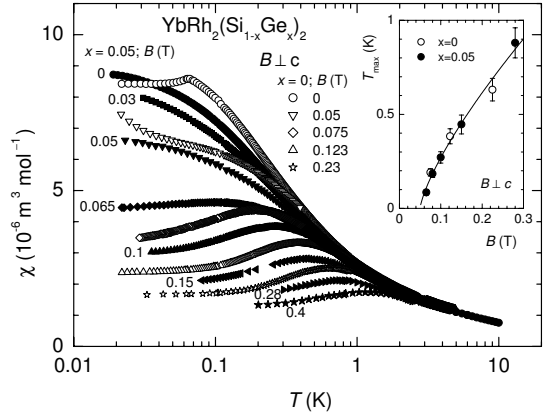Fig. 2. Comparison of ac-susceptibility data for YbRh$_2$(Si$_{1-x}$Ge$_x$)$_2$ (open symbols: $x = 0$, closed symbols: $x = 0.05$) at various fields applied perpendicular to the $c$-axis. Inset displays position of susceptibility maxima.

three-times lower Néel temperature results in a reduced critical field of about 0.027 mT.[4] The boundary of the AF phase for both systems, as derived from transport[5] and thermodynamic[11] measurements, is displayed in inset b of Fig. 1.

From the slope of the CW behavior, which persists at low fields up to 0.05 T (see inset a of Fig. 1), a large fluctuating moment of $\mu_{eff} \approx 1.4\mu_B$ per Yb$^{3+}$ is deduced.[4] Note, however, that these are not free moments. Their corresponding entropy $R\log 2$ is recovered only above 20 K[3] and the Weiss temperature of $\Theta \simeq -0.3$ K indicates a substantial antiferromagnetic coupling. At fields larger than 0.05 T the behavior changes drastically. This is displayed in Fig. 2: Upon cooling, $\chi(T)$ passes through a maximum followed by a $T^2$ dependence at low temperatures, indicating the formation of a field-induced LFL state also observed in specific heat and electrical resistivity measurements.[4] For fields larger than 0.06 T, i.e. the critical field for the undoped system, no major differences are resolved between the $x = 0$ and $x = 0.05$ system. The positions of the susceptibility maxima define a characteristic temperature that increases with increasing magnetic field (see inset of Fig. 2).

For $B \geq B_c$, the $T \to 0$ saturation values of $\chi(T)$ represent the Pauli-susceptibility, $\chi_0(B)$, which is strongly field dependent for this system.[10] When plotted against the field difference from the critical field, $B - B_c$, a divergent behavior, $\chi_0 \propto (B - B_c)^{-0.6}$ is found which indicates ferromagnetic quantum critical fluctuations.[10] This resembles the $T^{-0.6}$ divergence in the temperature dependence of the zero-field susceptibility. However, closest to the QCP, the bulk susceptibility remains finite, as evidenced by the CW behavior with non-vanishing Weiss temperature. A discussion of the origin of the line of susceptibility maxima shown in the inset of Fig. 2 will be given after the comparison with corresponding anomalies in the isothermal magnetization in the next section.

## 4. Magnetization

At first, we verify that the low-frequency (16.67 Hz) ac-susceptibility reflects the differential susceptibility for
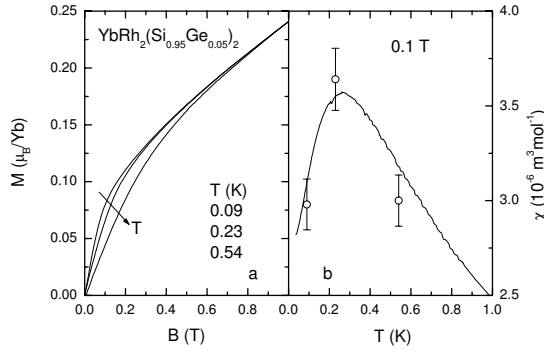
Fig. 3. a: Isothermal dc-magnetization for $YbRh_2(Si_{0.95}Ge_{0.05})_2$ at different temperatures. b: Comparison of the ac-susceptibility $\chi(T)$ at 0.1 T (line) with the differential magnetization $dM/dB$ (open circles), obtained at 0.1 T from the data shown in (a).



Fig. 5. Isothermal magnetization $M(B)$ (left axis) and susceptibility dM/dB (right axis) for $YRh_2(Si_{0.95}Ge_{0.05})_2$ for fields applied along the $c$-axis at 0.1 K.

$YbRh_2Si_2$ in the entire temperature-field range close to the QCP. Since we have not detected any out-of-phase component in the ac-susceptibility, the magnetization behavior should not show any hysteresis. Thus, the real part of the ac-susceptibility equals the differential bulk susceptibility $dM/dB$. Bulk magnetization measurements have been performed at various temperatures as a function of magnetic field. Fig. 3a shows that $M(B)$ is strongly nonlinear at small magnetic fields. The differential suscpetibility $dM/dB|_{T=const}$ obtained by numerical differentiation of the magnetization data at 0.1 T agrees with the real part of the ac-susceptibility registered continuously at this field. This is shown in Fig. 3b.
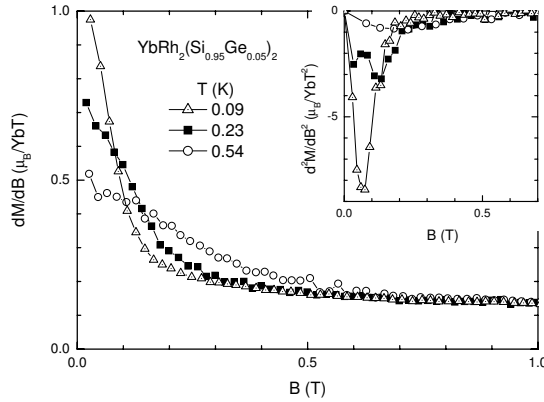


Fig. 4. Differential susceptibility $dM/dB$ vs $B$ ($B \perp c$) for $YRh_2(Si_{0.95}Ge_{0.05})_2$ at different temperatures. Inset displays temperature dependence of $d^2M/dB^2$.

As displayed in Fig. 4, the maximum change of slope in the isothermal magnetization $M(B)$ corresponds to a step-like decrease of the differential susceptibility $dM(B)/dB$ and a minimum in the second field-derivative $d^2M(B)/dB^2$. There is a clear relation between this anomaly and the maximum in the isofield ac-susceptibility data (compare Fig. 3b): the latter originates from the shift of the kink-like structure in $M(B)$ towards larger fields with increasing temperature. As will be shown in section 5, the positions of the maxima in
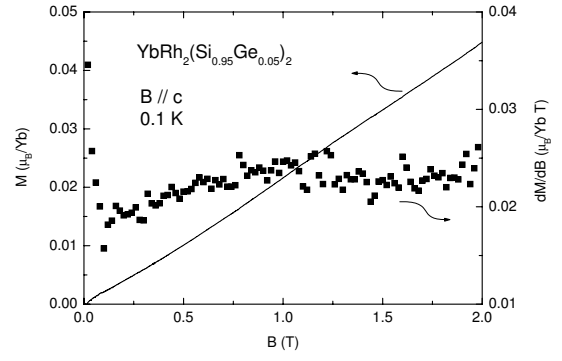
$\chi_{ac}(T)$ agree well with those of the inflection points in $dM(B)/dB$.

From the slope of the low-temperature magnetization, the field-dependence of the Pauli-susceptibility $\chi_0(B)$ has been determined.[10] For 0.3 T $\lesssim B \lesssim$ 10 T, the Pauli susceptibility is proportional to the Sommerfeld coefficient $\gamma(B)$, giving rise to a constant Sommerfeld-Wilson (SW) ratio of 17.5. This highly enhanced value indicates strong ferromagnetic fluctuations.[10]

It is very difficult to determine the magnetization along the hard direction, because the magnetic anisotropy is very large and amounts to about 100 at 0.1 K. The effect of the strong torque acting on the sample plate has been eliminated here, by comparing the forces with the gradient coils switched on and off. Due to the tiny value of the $c$-axis susceptibility, the background contribution of the magnetometer has to be carefully subtracted. As shown in Fig. 5, $M$ vs $B$ follows an almost linear dependence at very low temperatures. No clear structures as observed for fields perpendicular to the $c$-axis are resolved. Linear magnetization behavior $M(B) \propto B$ is observed at 0.5 K up to very high fields of 55 T.[12]
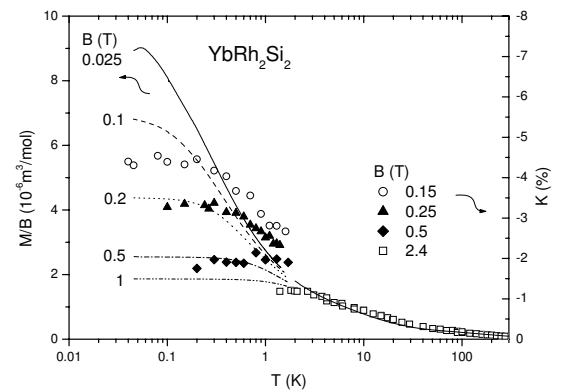


Fig. 6. Comparison of magnetization $M(T)/B$ (left axis) and [29]-Si-NMR derived Knight shift $K(T)$ (right axis, Ref.[13]) at various magnetic fields ($B \perp c$) for $YbRh_2Si_2$.

It has been shown by Ishida et al.,[13] that the Knight shift derived from ^{29}Si-NMR experiments is propor-

tional to the bulk magnetization, as expected from $K = (f_{res-}f_0)/f_0 = M(H)/B$ ($f_{res}$: resonance frequency, $f_0$: $K = 0$ position of the resonance). For paramagnets, the ratio $M/B$ equals the susceptibility $dM/dB$. In YbRh$_2$Si$_2$, however, the magnetization is strongly nonlinear at small fields. Indeed, the temperature dependences of $M(T)/B$ and $K(T)$, displayed in Fig. 6 are rather different from that of $\chi(T)$ (see Fig. 2). Whereas $\chi(T)$ at $B \geq B_c$ passes a characteristic maximum upon cooling, $M(T)/B$ and $K(T)$[13] both show monotonic behavior. We note, that the positions of the inflection points, i.e. the minima in the temperature derivative $dM(T)/dT$, are different from those of the susceptibility maxima shown in the inset of Fig. 2. As discussed in detail in Ref.,[14] the temperature derivative of the magnetization, $dM(T)/dT$, equals the field derivative of the entropy, $dS(T)/dB$, as expected from the Maxwell relation. The field dependence of the minimum in $dM(T)/dT$ varies linearly in $B - B_c$ and is clearly different from that of the maxima in $\chi(T)$.

The difference between the temperature dependence of the magnetization, $dM(T)/dT$, and that of the susceptibility, $\chi(T)$ is also reflected in the occurrence of temperature over field, $T/(B - B_c)$, scaling: Like for both the specific heat coefficient and the temperature derivative of the electrical resistivity,[4] such scaling behavior is observed for $dM/dT$.[14] By contrast, the susceptibility data do not show $T/(B - B_c)$ scaling.
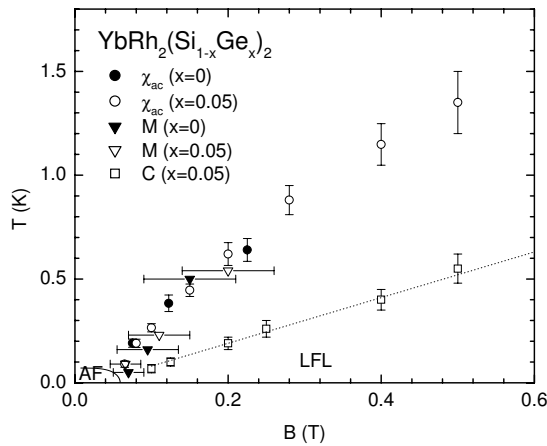
## 5. Phase diagram



Fig. 7. Temperature vs magnetic field phase diagram for YbRh$_2$(Si$_{1-x}$Ge$_x$)$_2$ (closed symbols: $x = 0$, open symbols: $x = 0.05$) for fields applied perpendicular to the $c$-axis. Circles and triangles indicate positions of maxima in ac-susceptibility $\chi(T)$ and inflection points of differential susceptibility $dM(B)/dB$, respectively. Squares mark positions of maxima in specific heat coefficient[4] which represent the upper limit of Landau Fermi liquid (LFL) behavior. Solid line indicates boundary of antiferromagnetic (AF) state in $x = 0$ system.[5]

Fig. 7 shows the $B - T$ phase diagram for YbRh$_2$(Si$_{1-x}$Ge$_x$)$_2$ ($x = 0$ and $x = 0.05$). For the crossover found in the magnetic properties, no differences between the two systems can be resolved within scattering

of the data. The main effect of Ge-substitution is the weakening of the AF ordered phase.

We now discuss the nature of this cross-over line. It is clearly separated from the line of maxima of the electronic specific heat coefficient $C_{el}(T)/T$ which indicates the boundary of the field-induced Landau Fermi liquid (LFL) state.[4] Upon passing the new magnetic cross-over line by increasing the magnetic field, the magnetization curve shows a considerable decrease in slope which indicates a partial ferromagnetic polarization of fluctuating moments.[10] Accordingly, with increasing field the characteristic temperature, at which this polarization sets in, in found to increase. Note, however, that a full polarization is only obtained beyond a field of 10 T which suppresses the HF state in YbRh$_2$Si$_2$.[9] In fact, the magnetization at the cross-over amounts to $0.1\mu_B/Yb$ only, i.e. less than 10% of the effective fluctuating moment of $1.4\mu_B/Yb$.

The analysis of $^{29}$Si-NMR data on YbRh$_2$Si$_2$ has revealed a two-component spectrum of quantum critical fluctuations.[13] Whereas the Knight shift, a local measure of the $\mathbf{q=0}$ fluctuations, saturates close to the QCP, the relaxation rate $(1/T_1)$ being proportional to a $\mathbf{q}$-average of the susceptibility, continues to grow. This disparity was considered a proof of the existence of AF quantum critical fluctuations in the intimate vicinity of the QCP which coexist with FM fluctuations. AF quantum critical fluctuations are also consistent with the observed CW behavior of the susceptibility in close vicinity to the QCP. On the other hand, for fields larger than the critical field, the AF component of the quantum critical fluctuations is suppressed, and FM fluctuations dominate as evidenced by the strongly enhanced SW ratio.

## 6. Summary

We have focused our attention on the magnetic properties of the field-tuned QCP in YbRh$_2$Si$_2$. The Sommerfeld-Wilson ratio is highly enhanced in the easy plane perpendicular to the $c$-axis, indicating pronounced FM fluctuations. A line of characteristic anomalies in both the temperature and field dependences of the susceptibility has been observed, which is different both from the boundary of the AF phase as well as from the border of the LFL state. This cross-over indicates a partial (less than 10%) polarization of fluctuating moments. On the other hand, CW behavior in the close vicinity to the critical field is compatible with an AF QCP. Most likely, the spectrum of the quantum critical fluctuations in YbRh$_2$Si$_2$ is complicated and consists of both, a zero- and finite-$\mathbf{q}$ component.

## Acknowledgment

1) S. Doniach, Physica **B 91**, 231 (1977).

2) P. Coleman, C. Pépin, Q. Si, R. Ramazashvili, J. Phys. Cond. Matt. **13**, R723 (2001).

3) O. Trovarelli, C. Geibel, S. Mederle, C. Langhammer, F.M. Grosche, P. Gegenwart, M. Lang, G. Sparn, F. Steglich, Phys. Rev. Lett. **85**, 626 (2000).

4) J. Custers, P. Gegenwart, H. Wilhelm, K. Neumaier, Y. Tokiwa, O. Trovarelli, C. Geibel, F. Steglich, C. Pépin, P. Coleman, Nature **424**, 524 (2003).

5) P. Gegenwart, J. Custers, C. Geibel, K. Neumaier, T. Tayama, K. Tenya, O. Trovarelli, F. Steglich, Phys. Rev. Lett. **89**, 056402 (2002).

6) R. Küchler, N. Oeschler, P. Gegenwart, T. Cichorek, K. Neumaier, O. Tegus, C. Geibel, J.A. Mydosh, F. Steglich, L. Zhu, Q. Si, Phys. Rev. Lett. **91**, 066405 (2003).

7) S. Paschen, T. Lühmann, S. Wirth, P. Gegenwart, O. Trovarelli, C. Geibel, F. Steglich , P. Coleman, Q. Si, Nature **432**, 881 (2004).

8) K. Ishida, D.E. MacLaughlin, O.O. Bernal, R.H. Heffner, G.J. Nieuwenhuys, O. Trovarelli, C. Geibel, F. Steglich, Physica B **326**, 403 (2003).

9) Y. Tokiwa, P. Gegenwart, T. Radu, J. Ferstl, G. Sparn, C. Geibel, F. Steglich, Phys. Rev. Lett. **94**, 226402 (2005).

10) P. Gegenwart, J. Custers, Y. Tokiwa, C. Geibel, F. Steglich, Phys. Rev. Lett. **94**, 076402 (2005).

11) R. Küchler, F. Weickert, P. Gegenwart, N. Oeschler, J. Ferstl, C. Geibel, F. Steglich, J. Magn. Magn. Mat. **272-276**, 229 (2004).

12) P. Gegenwart, J. Custers, T. Tayama, K. Tenya, C. Geibel, G. Sparn, N. Harrison, P. Kerschl, D. Eckert, K.-H. Müller, F. Steglich, J. Low Temp. Phys. **133**, 3 (2003).

13) K. Ishida, K. Okamoto, Y. Kawasaki, Y. Kitaoka, O. Trovarelli, C. Geibel, F. Steglich, Phys. Rev. Lett. **89**, 107202 (2002).

14) P. Gegenwart, Y. Tokiwa, K. Neumaier, C. Geibel, F. Steglich, Physica **B 359-361**, 23 (2005).